WORST CASE ANALYSIS OF DECENTRALIZED KALMAN FILTERS UNDER COMMUNICATION CONSTRAINTS

M.S. Schlosser and K. Kroschel

Institut für Nachrichtentechnik, Universität Karlsruhe
Kaiserstr. 12, 76128 Karlsruhe, GERMANY
phone: +49-721-608-3348, fax: +49-721-606-3799, email: schlosser@int.uni-karlsruhe.de
web: http://www.int.uni-karlsruhe.de/~schlosse/

ABSTRACT

Decentralized Kalman filters are often used in multi-sensor target tracking as such a distributed fusion architecture has several advantages compared with centralized ones. On the other hand, distributed fusion is not only conceptually more complex but the required bandwidth is also likely to be a lot higher. However, a trade-off between bandwidth and performance is possible. In this work, the worst case performance degradation due to a reduction in communication rate between the processing nodes of a decentralized Kalman filter is derived analytically and verified by simulations.

1. INTRODUCTION

In multi-sensor target tracking a centralized fusion architecture was used traditionally where all the data from the different sensors is sent to a single location to be fused. In recent years, increasing emphasis has been placed on distributed fusion where several fusion nodes exist in the network, like e.g. the Decentralized Kalman Filter (DKF).

The advantages of such a distributed fusion architecture are a higher robustness due to redundancy of fusion nodes and a lower processing load at each fusion node. For a large number of sensors, centralized fusion might not even be applicable at all if the central processor or the network cannot handle the large amount of data transmitted by the sensors.

On the other hand, distributed fusion is not only conceptually more complex but the required bandwidth is also likely to be a lot higher compared with centralized fusion. However, in contrast to centralized fusion, a trade-off between bandwidth and performance is possible by letting the fusion nodes communicate at reduced rates. In this case, the performance degrades as the information conveyed by the different local processors becomes correlated due to propagating the same underlying process noise [1, 2].

In [1], a formula for the steady-state performance of a DKF was derived and compared with simulative results for two sensors and a constant velocity model for the target dynamics. In this work a simple formula for the performance degradation in the worst case of ignoring the correlation completely is derived whose evaluation is straightforward compared with the solution of the asymmetric Lyapunov equation in [1]. Furthermore, the simulative study is extended to a constant acceleration model and its implications. To keep the treatment simple, we also want to focus on communication issues in a simple DKF consisting of two Local Kalman Filters (LKFs) producing track estimates based on a single local Sensor (S) and a Fusion Center (FC) combining these local estimates to a global one, as depicted in Fig. 1.

This paper is organized as follows: The DKF is introduced in Sect. 2. Sect. 3 provides the theoretical background on why the DKF requires more communication bandwidth and on how it can be reduced. In Sect. 4, the performance degradation for the worst case of ignoring the correlation between the local estimates completely is derived and validated by simulations. Finally, Sect. 5 draws some conclusions.

This work is part of the Sonderforschungsbereich (SFB) No. 588 *"Humanoide Roboter - Lernende und kooperierende multimodale Roboter"* at the University of Karlsruhe. The SFB is supported by the Deutsche Forschungsgemeinschaft (DFG).

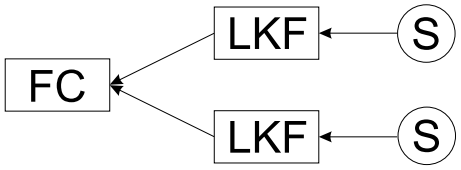

Figure 1: DKF for two sensors

2. DECENTRALIZED KALMAN FILTER

For a Kalman Filter (KF) to be applicable, the target's dynamics need to be modeled by the following state space equation

$$\mathbf{x}(k+1) = \mathbf{F}\mathbf{x}(k) + \mathbf{w}(k), \tag{1}$$

where $\mathbf{x}(k)$ is the state vector of the target at time instant k, typically containing the target position, velocity etc. $\mathbf{F}$ is the time-invariant state transition matrix and $\mathbf{w}(k)$ a white noise sequence with covariance matrix $\mathbf{Q}(k)$ representing the process noise.

Respectively, the linear measurement models are given by

$$\mathbf{y}_i(k) = \mathbf{H}_i\mathbf{x}(k) + \mathbf{v}_i(k), \tag{2}$$

where $\mathbf{y}_i(k)$ is the observation vector of the i^{th} sensor, $i = 1,\ldots,N$. In our case, $N = 2$ sensors measure the position of the target. $\mathbf{H}_i$ is the corresponding measurement matrix and $\mathbf{v}_i(k)$ a zero-mean, white noise sequence with covariance matrix $\mathbf{R}_i(k)$ representing the measurement noise.

According to these model equations, the *centralized* KF (CKF) algorithm in its information form with multiple inputs can be described as recursively performing the following two steps to calculate the overall position estimate $\hat{\mathbf{x}}_{\text{CKF}}(k|k)$ and error covariance matrix $\mathbf{P}_{\text{CKF}}(k|k)$ at time instant k [3]:
1. Prediction

$$\hat{\mathbf{x}}_{\text{CKF}}(k|k-1) = \mathbf{F}\hat{\mathbf{x}}_{\text{CKF}}(k-1|k-1) \tag{3}$$

$$\mathbf{P}_{\text{CKF}}(k|k-1) = \mathbf{F}\mathbf{P}_{\text{CKF}}(k-1|k-1)\mathbf{F}^T + \mathbf{Q}(k-1) \tag{4}$$

2. Estimate correction

$$\hat{\mathbf{x}}_{\text{CKF}}(k|k) = \mathbf{P}_{\text{CKF}}(k|k)\Big(\mathbf{P}^{-1}_{\text{CKF}}(k|k-1)\hat{\mathbf{x}}_{\text{CKF}}(k|k-1) + \sum_{i=1}^{N}\mathbf{H}_i^T\mathbf{R}_i^{-1}(k)\mathbf{y}_i(k)\Big) \tag{5}$$

$$\mathbf{P}^{-1}_{\text{CKF}}(k|k) = \mathbf{P}^{-1}_{\text{CKF}}(k|k-1) + \sum_{i=1}^{N}\mathbf{H}_i^T\mathbf{R}_i^{-1}(k)\mathbf{H}_i. \tag{6}$$

This is called the information form as the inverse of the covariance matrix $\mathbf{P}^{-1}$ is a measure for the accuracy of the corresponding state estimate $\hat{\mathbf{x}}$ and thus for the information contained in it. As described by Eq. (5), $\mathbf{P}^{-1}(k|k-1)$ determines the weight given to $\hat{\mathbf{x}}(k|k-1)$.

In the *decentralized* KF (DKF), the LKFs produce estimates $\hat{\mathbf{x}}_i(k|k)$ based on the information available from a single sensor i using the standard KF equations, i.e. Eqs. (3-6) with $N=1$. At the FC, these estimates are fused together to form the overall state estimate $\hat{\mathbf{x}}_{\text{DKF}}(k|k)$ [2] (see Fig. 1)

$$\hat{\mathbf{x}}_{\text{DKF}}(k|k) = \mathbf{P}_{\text{DKF}}(k|k)\Big(\mathbf{P}^{-1}_{\text{DKF}}(k|k-1)\hat{\mathbf{x}}_{\text{DKF}}(k|k-1) + \sum_{i=1}^{N}\left[\mathbf{P}_i^{-1}(k|k)\hat{\mathbf{x}}_i(k|k) - \mathbf{P}_i^{-1}(k|k-1)\hat{\mathbf{x}}_i(k|k-1)\right]\Big) \tag{7}$$

$$\mathbf{P}^{-1}_{\text{DKF}}(k|k) = \mathbf{P}^{-1}_{\text{DKF}}(k|k-1) + \sum_{i=1}^{N}\left[\mathbf{P}_i^{-1}(k|k) - \mathbf{P}_i^{-1}(k|k-1)\right], \tag{8}$$

where $\mathbf{P}_{\text{DKF}}$ and $\mathbf{P}_i$ are the error covariance matrices of the state estimates $\hat{\mathbf{x}}_{\text{DKF}}$ at the FC and $\hat{\mathbf{x}}_i$ at the LKFs, respectively.

The state estimate $\hat{\mathbf{x}}_{\text{DKF}}(k|k)$ in Eq. (7) can be shown to be equivalent to $\hat{\mathbf{x}}_{\text{CKF}}(k|k)$ in Eq. (5): Solving Eq. (5) adapted to the single sensor case, i.e. $N=1$, for the weighted measurement $\mathbf{H}_i^T\mathbf{R}_i^{-1}(k)\mathbf{y}_i(k)$ leads to the equivalence between $\mathbf{H}_i^T\mathbf{R}_i^{-1}(k)\mathbf{y}_i(k)$ in Eq. (5) and the gain in information between the predicted local estimates $\hat{\mathbf{x}}_i(k|k-1)$ and the corrected ones $\hat{\mathbf{x}}_i(k|k)$ in Eq. (7)

$$\mathbf{H}_i^T\mathbf{R}_i^{-1}(k)\mathbf{y}_i(k) = \mathbf{P}_i^{-1}(k|k)\hat{\mathbf{x}}_i(k|k) - \mathbf{P}_i^{-1}(k|k-1)\hat{\mathbf{x}}_i(k|k-1). \tag{9}$$

3. COMMUNICATION CONSTRAINTS

In a distributed fusion network the required bandwidth is likely to be a lot higher compared with a centralized architecture. First, the information packages in a DKF are larger as the state vector usually is of a higher dimension compared with the measurement vector. Second, for realistic applications with many sensors a distributed fusion architecture with several fusion nodes is used typically. Thus, many more nodes exist in the network, which need to communicate with each other. This is especially important if the final estimate shall be obtained at several fusion nodes. Therefore, constraints on communication bandwidth are an important issue in DKFs.

On the other hand, centralized fusion might not even be applicable at all for a large number of sensors if the central processor or the network cannot handle the large amount of data transmitted by the sensors. In this case, the DKF opens up the possibility to distribute the processing load and to save the necessary bandwidth by letting the LKFs communicate with the FC less frequently. The update rate at the LKFs is, however, not affected. The LKFs still run at the sensor observation rate.

Reducing the communication rate by a factor m results in all predictions by one step being replaced with predictions by m steps in Eqs. (7,8). The predictions, however, account for the common history of the local estimates $\hat{\mathbf{x}}_i(k|k)$. The different $\hat{\mathbf{x}}_i(k|k)$ are correlated due to propagating the same underlying process noise $\mathbf{w}(k)$ in Eq. (1) [4]. If the predictions by one step are replaced by predictions by m steps, the correlation that has been built up since the last update cannot be removed during the fusion process, and the performance of the DKF degrades [1, 2]. On the other hand, if $\mathbf{w}(k)=\mathbf{0}$, i.e. the target's dynamics can be modeled exactly, the local estimates $\hat{\mathbf{x}}_i(k|k)$ are not correlated and, therefore, the communication rate can be reduced at will without any performance degradation.

For less and less frequent communication between the LKFs and the FC, i.e. $m\to\infty$, the information contained in the predicted state estimates becomes less and less reliable. This is represented by the inverses of the corresponding error covariance matrices $\mathbf{P}^{-1}_{\text{DKF}}(k|k-m)$ and $\mathbf{P}_i^{-1}(k|k-m)$ approaching zero. Thus, no weight is given to these estimates and they can be discarded in Eqs. (7, 8) leading to

$$\hat{\mathbf{x}}_{\text{simple}}(k|k) = \mathbf{P}_{\text{simple}}(k|k)\sum_{i=1}^{N}\mathbf{P}_i^{-1}(k|k)\hat{\mathbf{x}}_i(k|k) \tag{10}$$

$$\mathbf{P}^{-1}_{\text{simple}}(k|k) = \sum_{i=1}^{N}\mathbf{P}_i^{-1}(k|k). \tag{11}$$

This is equivalent to a simple fusion architecture that assumes the local state estimates $\hat{\mathbf{x}}_i(k|k)$ and $\hat{\mathbf{x}}_j(k|k)$ to be statistically independent for all $i\neq j$. Therefore, the estimate $\hat{\mathbf{x}}_{\text{simple}}(k|k)$ can serve as a worst case scenario. More frequent communication necessarily leads to better estimates.

4. SIMPLE FUSION ARCHITECTURE

In this section the performance degradation due to ignoring the correlation between the local estimates is investigated in detail. First, the performance of the $\text{DKF}_{\text{simple}}$ defined by Eqs. (10, 11) is derived analytically. Second, the analytical performance is compared with simulative results.

4.1 Analytical Performance Analysis

Introducing $\tilde{\mathbf{x}}_*(k|k) = \hat{\mathbf{x}}_*(k|k) - \mathbf{x}(k)$ in Eq. (10), where * either stands for "simple" or i, and after some algebraic manipulations, it follows for the true covariance $\mathbf{P}_{\text{true}}(k|k) = \text{E}\left\{\tilde{\mathbf{x}}_{\text{simple}}(k|k)\tilde{\mathbf{x}}^T_{\text{simple}}(k|k)\right\}$ of the $\text{DKF}_{\text{simple}}$

$$\mathbf{P}_{\text{true}}(k|k) = \mathbf{P}_{\text{simple}}(k|k) + \mathbf{P}_{\text{simple}}(k|k) \cdot \Big(\sum_{i=1}^{N}\sum_{\substack{j=1\\ j\neq i}}^{N}\mathbf{P}_i^{-1}(k|k)\mathbf{\Sigma}_{i,j}(k|k)\mathbf{P}_j^{-1}(k|k)\Big)\mathbf{P}_{\text{simple}}(k|k). \tag{12}$$

where the cross-covariance $\mathbf{\Sigma}_{i,j}(k|k) = \text{E}\left\{\tilde{\mathbf{x}}_i(k|k)\tilde{\mathbf{x}}_j^T(k|k)\right\}$ between two local estimates can be determined using [4]

$$\mathbf{\Sigma}_{i,j}(k|k) = (\mathbf{I}-\mathbf{K}_i(k)\mathbf{H}_i)\cdot(\mathbf{F}\mathbf{\Sigma}_{i,j}(k-1|k-1)\mathbf{F}^T + \mathbf{Q})\cdot(\mathbf{I}-\mathbf{K}_j(k)\mathbf{H}_j)^T. \tag{13}$$

$\mathbf{I}$ denotes the identity matrix and $\mathbf{K}_i(k)$ as well as $\mathbf{K}_j(k)$ the Kalman gains.

The worst case that all sensors are equal, i.e. $\mathbf{P}_i(k|k) =: \mathbf{P}_{\text{LKF}}(k|k)\ \forall i$, also results in $\mathbf{\Sigma}_{i,j}(k|k) = \mathbf{\Sigma}_{j,i}(k|k) =: \mathbf{\Sigma}_{\text{LKFs}}(k|k)\ \forall i,j$. Therefore, the true covariance simplifies to

$$\mathbf{P}_{\text{true}}(k|k) = \frac{1}{N}\mathbf{P}_{\text{LKF}}(k|k) + \frac{N-1}{N}\mathbf{\Sigma}_{\text{LKFs}}(k|k), \tag{14}$$

as $\mathbf{P}_{\text{simple}}(k|k) = \frac{1}{N}\mathbf{P}_{\text{LKF}}(k|k)$. The evaluation of Eqs. (12, 14) is straightforward compared with the solution of the asymmetric Lyapunov equation describing the steady-state performance of a DKF for arbitrary communication rates in [1].

4.2 Simulative Validation

This theoretical performance of the $\text{DKF}_{\text{simple}}$ is now compared with simulative results. For simplicity the comparison is restricted to 1D models and the case of $N=2$ identical sensors, which measure the position in Cartesian coordinates

$$y_i(k) = x(k) + v_i(k), \quad i=1,2 \tag{15}$$

with equal variances $\sigma^2_{v,i} = \sigma^2_v$. 1000 Monte Carlo runs with 400 measurements per simulation were performed. The averages, however, are only based on the last 200 measurements to obtain an estimate of the steady-state performance.

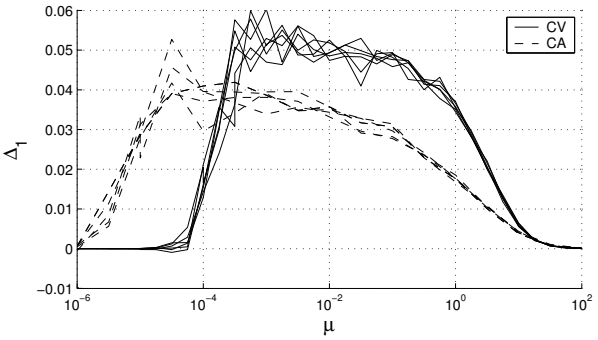

Figure 2: Relative difference between $\mathrm{MSE}_{\mathrm{simple}}$ and $\mathrm{MSE}_{\mathrm{DKF}}$ as a function of the target maneuvering index μ for the constant velocity (CV) and the constant acceleration (CA) model ($T_s = 0.1\,\mathrm{s}, 1\,\mathrm{s}, 10\,\mathrm{s}$; $\sigma_v = 0.1\,\mathrm{m}, 1\,\mathrm{m}, 10\,\mathrm{m}$)

In [5], the case of a Constant Velocity (CV) model has already been examined. The CV model, which is excited by discretized continuous-time white noise, is defined by

$$\begin{bmatrix} x(k+1) \\ \dot{x}(k+1) \end{bmatrix} = \begin{bmatrix} 1 & T_s \\ 0 & 1 \end{bmatrix} \begin{bmatrix} x(k) \\ \dot{x}(k) \end{bmatrix} + \mathbf{w}_{\mathrm{CV}}(k)\,, \tag{16}$$

where T_s denotes the sampling period and

$$\mathbf{w}_{\mathrm{CV}}(k) = \int_0^{T_s} \begin{bmatrix} T_s - t \\ 1 \end{bmatrix} u_{\mathrm{CV}}(kT_s + t)\,dt \tag{17}$$

with $u_{\mathrm{CV}}(t)$ being a zero-mean continuous random noise sequence with power spectral density $N_{0,\mathrm{CV}}$. It was found that the relative difference

$$\Delta_1 = \frac{\mathrm{MSE}_{\mathrm{simple}} - \mathrm{MSE}_{\mathrm{DKF}}}{\mathrm{MSE}_{\mathrm{DKF}}} \stackrel{!}{=} \frac{P^{11}_{\mathrm{true}} - P^{11}_{\mathrm{DKF}}}{P^{11}_{\mathrm{DKF}}} \tag{18}$$

(P^{11} indicates the upper left element of matrix $\mathbf{P}$) between the Mean Square Error (MSE) in the position estimate of the $\mathrm{DKF}_{\mathrm{simple}}$ and the DKF is invariant with respect to varying sampling periods T_s and measurement noises σ_v (see Fig. 2) if plotted against the target maneuvering index [3]

$$\mu_{\mathrm{CV}} = \sqrt{\frac{N_{0,\mathrm{CV}} T_s^3}{\sigma_v^2}}\,. \tag{19}$$

In Fig. 2, it can be seen as well that the curves for Δ_1 are also invariant with respect to varying sampling periods T_s and measurement noises σ_v if plotted against the target maneuvering index

$$\mu_{\mathrm{CA}} = \sqrt{\frac{N_{0,\mathrm{CA}} T_s^5}{\sigma_v^2}} \tag{20}$$

for the Constant Acceleration (CA) model

$$\begin{bmatrix} x(k+1) \\ \dot{x}(k+1) \\ \ddot{x}(k+1) \end{bmatrix} = \begin{bmatrix} 1 & T_s & \frac{1}{2}T_s^2 \\ 0 & 1 & T_s \\ 0 & 0 & 1 \end{bmatrix} \begin{bmatrix} x(k) \\ \dot{x}(k) \\ \ddot{x}(k) \end{bmatrix} + \mathbf{w}_{\mathrm{CA}}(k)\,, \tag{21}$$

where

$$\mathbf{w}_{\mathrm{CA}}(k) = \int_0^{T_s} \begin{bmatrix} \frac{1}{2}(T_s - t)^2 \\ T_s - t \\ 1 \end{bmatrix} u_{\mathrm{CA}}(kT_s + t)\,dt \tag{22}$$

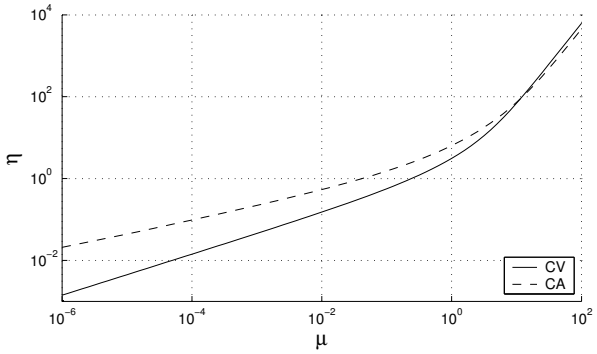

Figure 3: Relationship between the target maneuvering index μ and the weighting ratio η

and $u_{\mathrm{CA}}(t)$ is again a zero-mean continuous random noise sequence with power spectral density $N_{0,\mathrm{CA}}$. On the other hand, the curves for the CA model and those for the CV model clearly do not match.

The CV and CA motion models lead to the following process noise covariance matrices [3]

$$\mathbf{Q}_{\mathrm{CV}} = \begin{bmatrix} \frac{1}{3}T_s^3 & \frac{1}{2}T_s^2 \\ \frac{1}{2}T_s^2 & T_s \end{bmatrix} N_{0,\mathrm{CV}} \tag{23}$$

and

$$\mathbf{Q}_{\mathrm{CA}} = \begin{bmatrix} \frac{1}{20}T_s^5 & \frac{1}{8}T_s^4 & \frac{1}{6}T_s^3 \\ \frac{1}{8}T_s^4 & \frac{1}{3}T_s^3 & \frac{1}{2}T_s^2 \\ \frac{1}{6}T_s^3 & \frac{1}{2}T_s^2 & T_s \end{bmatrix} N_{0,\mathrm{CA}}\,. \tag{24}$$

As expressed by Eq. (4), $Q^{11}_{\mathrm{CV}} = \frac{1}{3}N_0 T_s^3$ and $Q^{11}_{\mathrm{CA}} = \frac{1}{20}N_0 T_s^5$ are the variances of the predicted position estimate due to the process noise for the two dynamics models, respectively. Therefore, μ is an indicator for the ratio between the weight given to the measurement and that given to the predicted estimate during the track update in the LKFs, as indicated in Eq. (5) for $N = 1$.

On the other hand, the accuracy of the prediction in the LKFs does not only depend on the process noise but also on the state transition matrix $\mathbf{F}$, as also described in Eq. (4). The exact ratio

$$\eta = \frac{P^{11}_{\mathrm{LKF,pred}}}{\sigma_v^2} \tag{25}$$

between the weight given to the measurement and that given to the predicted position estimate can either be taken from the simulations or, in the steady-state, it can also be calculated by solving a system of non-linear equations. The corresponding equations for a KF using a CV model are given in [3]. Those for the CA model can be derived accordingly.

The relationship between the target maneuvering index μ and the weighting ratio η is displayed in Fig. 3 and the resulting curves for the relative difference Δ_1 as a function of η in Fig. 4, where the bold lines present the analytical predictions. This time the curves for the CV and the CA model show the same progression. Only the maximum degradation for the CA model of around 4 % is lower than the 5 % for the CV model, as also predicted by the theory. This can be explained by the same η being reached for a smaller process noise resulting in a lower correlation between the local estimates.

For small values of η, the theory predicts Δ_1 to stay at its maximum, whereas the simulations show Δ_1 to approach zero. This significant difference can be explained by the analytical curve predicting the steady-state behavior, whereas the steady-state is never reached during the simulations for such low values of η. As depicted in Fig. 5, the cross-covariance $\mathbf{\Sigma}_{i,j}(k|k)$ in Eq. (13) between

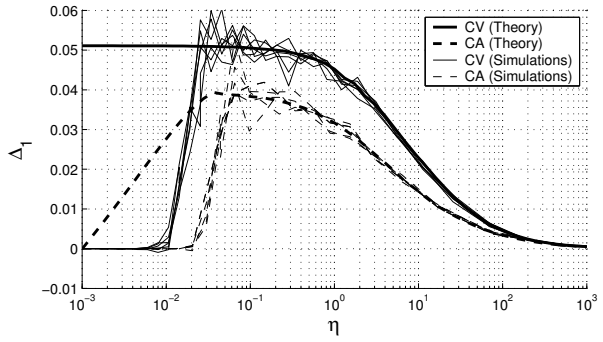

Figure 4: Relative difference between $\mathrm{MSE}_{\mathrm{simple}}$ and $\mathrm{MSE}_{\mathrm{DKF}}$ as a function of the weighting ratio η ($T_s = 0.1\,\mathrm{s}, 1\,\mathrm{s}, 10\,\mathrm{s}$; $\sigma_v = 0.1\,\mathrm{m}, 1\,\mathrm{m}, 10\,\mathrm{m}$)

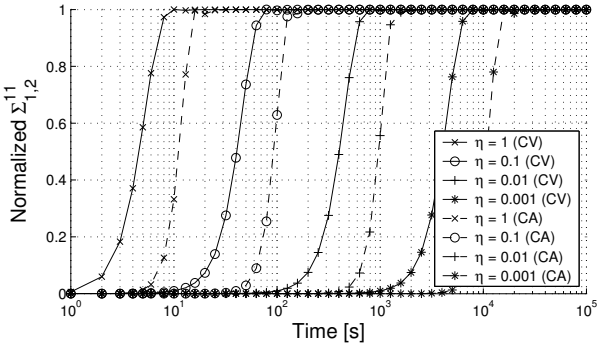

Figure 5: Time dependency of the normalized cross-covariance between the local position estimates

the local estimates rises only slowly for low values of η. The lacking cross-covariance renders Eqs. (10, 11) of the $\mathrm{DKF}_{\mathrm{simple}}$ quasi exact, the estimates $\hat{\mathbf{x}}_{\mathrm{DKF}}(k|k)$ and $\hat{\mathbf{x}}_{\mathrm{simple}}(k|k)$ identical, and Δ_1 zero during the initialization phase.

For small values of η, even the analytical prediction of the performance degradation fails for the CA case. This is due to the numerical solution of the system of non-linear equations for the steady-state filter performance reaching its limits in accuracy for such values of η. Simulations with 10000 measurements indicate that Δ_1 stays at its maximum also in the CA case.

KFs do not only produce state estimates $\hat{\mathbf{x}}$ but also calculate an accuracy of these estimates in form of the error covariance matrix $\mathbf{P}$. The DKF estimates its accuracy correctly whereas the $\mathrm{DKF}_{\mathrm{simple}}$, although performing slightly worse, estimates its accuracy even higher than that of the DKF. Fig. 6 shows this difference

$$\Delta_2 = \frac{\mathrm{MSE}_{\mathrm{simple}} - \mathrm{MSE}_{\mathrm{estimated}}}{\mathrm{MSE}_{\mathrm{estimated}}} \stackrel{!}{=} \frac{P^{11}_{\mathrm{true}} - P^{11}_{\mathrm{simple}}}{P^{11}_{\mathrm{simple}}} \qquad (26)$$

between the true and estimated MSE of the $\mathrm{DKF}_{\mathrm{simple}}$ as a function of the weighting ratio η. Again, the bold lines indicate the analytical prediction. The shape of these curves is very similar to those in Fig. 4 for the difference between the true MSE of the $\mathrm{DKF}_{\mathrm{simple}}$ and the DKF. The maxima are only higher at 16 % and 25 %, respectively. It can again be seen how this differences can be predicted very precisely by Eq. (14).

Note further that in Figs. 4 and 6 the variance in estimating Δ_1 and Δ_2 becomes bigger for smaller values of η. This increase in variance is due to the errors of the state estimate of a KF becoming more correlated in time for such values of η. Thus, the effective

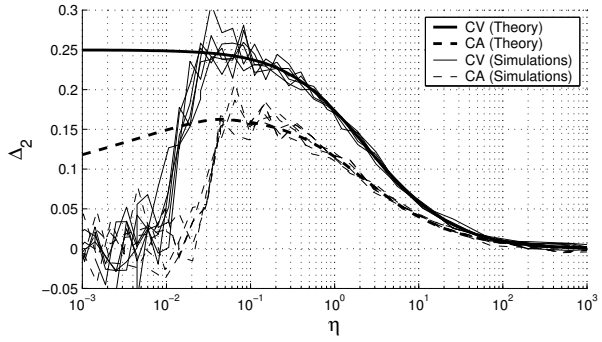

Figure 6: Relative difference between true and estimated MSE of $\mathrm{DKF}_{\mathrm{simple}}$ as a function of the weighting ratio η ($T_s = 0.1\,\mathrm{s}, 1\,\mathrm{s}, 10\,\mathrm{s}$; $\sigma_v = 0.1\,\mathrm{m}, 1\,\mathrm{m}, 10\,\mathrm{m}$)

number of samples is reduced on which the average in Eqs. (18) and (26) is performed.

On the other hand, in Fig. 4 the variance drops down to zero along with Δ_1 while in Fig. 6 for Δ_2 it keeps increasing for ever smaller values of η. This can be explained by $\hat{\mathbf{x}}_{\mathrm{DKF}}(k|k)$ and $\hat{\mathbf{x}}_{\mathrm{simple}}(k|k)$ becoming identical due to the lacking cross-correlation during the initialization phase for these values of η. Therefore, $\mathrm{MSE}_{\mathrm{simple}}$ and $\mathrm{MSE}_{\mathrm{DKF}}$ estimated with the help of the Monte Carlo simulations are exactly the same in calculating Δ_1. The self-assessment of the $\mathrm{DKF}_{\mathrm{simple}}$, as expressed by $\mathrm{MSE}_{\mathrm{estimated}}$, is, however, deterministic and, therefore, only becomes a correct estimate of estimated $\mathrm{MSE}_{\mathrm{simple}}$ but not identical with it in calculating Δ_2.

5. CONCLUSIONS

If the communication rate between the LKFs and the FC needs to be reduced to save bandwidth or processing load, the performance of the fusion process degrades as the information provided by the different sensors becomes correlated due to propagating the same underlying process noise. In this paper the worst case of ignoring this correlation completely is studied. A simple formula for the performance degradation is derived and validated by simulations. Its evaluation is straightforward compared with the solution of the asymmetric Lyapunov equation for the general case. Furthermore, it is shown that the ratio η between the weight given to the measurement and that given to the predicted position estimate during the track update in the LKFs is more meaningful than the target maneuvering index μ in describing the performance degradation.

REFERENCES

[1] K. C. Chang, T. Zhi, and R. K. Saha. Performance Evaluation of Track Fusion With Information Matrix Filter. *IEEE Transactions on Aerospace and Electronic Systems*, 38(2):455–466, 2002.

[2] M. E. Liggins, C.-Y. Chong, I. Kadar, M. G. Alford, V. Vannicola, and S. Thomopoulos. Distributed Fusion Architectures and Algorithms for Target Tracking. *Proceedings of the IEEE*, 85(1):95–107, Jan 1997.

[3] Y. Bar-Shalom and T. Fortmann. *Tracking and Data Association*. New York: Academic Press, 1988.

[4] Y. Bar-Shalom. On the Track-to-Track Correlation Problem. *IEEE Transactions on Automatic Control*, 26(2):571–572, 1981.

[5] M. S. Schlosser and K. Kroschel. Communication issues in decentralized Kalman filters. In *Int. Conf. on Information Fusion (Fusion 2004)*, pages 731–738, 2004.